

Received June 4, 2018, accepted July 13, 2018, date of publication July 20, 2018, date of current version August 15, 2018.

Digital Object Identifier 10.1109/ACCESS.2018.2857802

Adaptive Finite-Time Synchronization Control for Teleoperation System With Varying Time Delays

HAOCHEN ZHANG^{1,2}, AIGUO SONG^{ID}¹, (Senior Member, IEEE), AND SHAOBO SHEN¹

¹School of Instrument Science and Engineering, Southeast University, Nanjing 210096, China

²College of Electrical and Information Engineering, Lanzhou University of Technology, Lanzhou 730050, China

Corresponding author: Aiguo Song (a.g.song@seu.edu.cn)

This work was supported in part by the National Key Research and Development Program of China under Grant 2016YFB1001301 and in part by the National Natural Science Foundation of China under Grant 91648206 and Grant U1713210.

ABSTRACT In practical application, the synchronization tracking of teleoperation system requires the fast speed and strong robustness. It is the ideal control effect that the synchronization errors between master and slave robots can converge to zero in finite time. In this paper, we propose the new nonsingular terminal sliding mode and the adaptive finite-time control method for position tracking in teleoperation system. First, a novel nonsingular terminal sliding mode is designed to provide higher tracking precision and robustness. Second, the radial basis function neural networks are applied to solve dynamic uncertainties, and the adaptive laws are proposed to estimate the uncertain parameters and upper bounds of estimation. Then, the corresponding finite-time controllers of master and slave robots are designed. Third, based on the Lyapunov stability theory, synchronization performances of the closed-loop system are proved to be stable state and finite time. Finally, simulations are achieved, and some comparisons with two nonsingular terminal sliding mode control schemes and two PD methods are shown. The simulation results verify the effectiveness of the proposed control laws.

INDEX TERMS Teleoperation system, finite-time control, nonsingular terminal sliding mode, adaptive control, varying time delay.

I. INTRODUCTION

Teleoperation system extends the capability of human operation in an unknown and dangerous environment. A typical teleoperation system consists of the master robot, remote slave robot, a human operator, task environment and communication channel connecting with master and slave side. Providing stable position synchronization and environmental force feedback are the essential performance in controlled teleoperation systems. Moreover, synchronization control performance is very important for teleoperation system and has been widely investigated in many research works [1]. In practical teleoperation system, external disturbance, indeterminate and nonlinear dynamic model, communication time-delay are unavoidable problems, and these issues need to be considered in position synchronization controller design [2], [3].

Many control structures and control algorithms have been proposed to overcome these issues. Anderson and Spong [4] applied the passivity control approach based on scattering theory to stabilize the system with communication time delays. Niemeyer and Slotine [5] introduced the

wave-variables structure based on scattering theory to improve the time delay communication channel as the passive part. And then, some improved wave-variable architectures were proposed for synchronization tracking in teleoperations [6]–[8]. Furthermore, many other control structures and methods were introduced to handle position tracking problems in teleoperation system with communication time delays, such as fuzzy control [9], adaptive control [10]–[14], robust control [15], state feedback control based on Lyapunov-Krasovskii stability theory [16]–[18] and sliding mode control.

The sliding mode (SM) control method has been used in controlling various nonlinear systems. Many literature and research works introduced the SM for trajectory tracking control of robotic manipulators. However, the system states cannot achieve finite-time convergence in traditional SM control [19]. The terminal sliding mode (TSM) control was proposed to perform the convergence of system states in finite-time [20]. In recent years, many improved TSM control methods have been applied to tracking control of manipulators [19], [21]–[23]. In addition, the SM control and related

improvement algorithms have also been used in teleoperation systems. In literature [24], the sliding mode control was proposed for telerobot system with communication delay. Yang *et al.* [25]–[27] designed three fast nonsingular finite-time control schemes based on TSM for teleoperation system with constant communication delay to make the synchronization error of teleoperation system quickly converge to zero in finite-time, respectively. In [25] a novel switching terminal sliding mode surface was designed, and fuzzy logic systems were introduced to approximate the uncertain part of dynamic in teleoperation robots. In [26] the new error transformed variables were considered in TSM design, and the neural networks were applied for uncertain approximation. In [27], a nonsingular terminal sliding mode (NTSM) was designed and a finite-time control strategy was presented for teleoperation system under communication delay.

Although TMS based finite-time methods have been applied in teleoperation controllers design and have achieved the fast regulation speed, there are still some problems need to be improved. For one thing, the time delays of teleoperation communication channel in those work [24]–[27] are all constants, but actually, the time delays are time-varying in system. For another, as the sliding mode structures mentioned in above literature are composed of synchronous errors and error differential forms, the dynamic performance characteristics of the system could be loosed under varying communication delays and operator force effect. Recently, the integral TSM has been used in robot manipulators with higher steady-state tracking precision and robustness [28]. Zhao *et al.* [29] proposed integral SM control to guarantee synchronization control stability for bilateral teleoperation system. But in [29], time-varying delays and finite-time convergence are not considered.

In this paper, the adaptive finite-time control based on NTSM is proposed for synchronization control of teleoperation system under varying time delays and uncertain dynamic parameters. The designed sliding mode consists integral term of synchronization errors to improve the stability and dynamic performance of the control process. The master and slave controllers are designed based on nonsingular TSM method. The Radial Basis Function (RBF) neural networks are introduced to approximate the uncertainties in teleoperation dynamics. The adaptive laws with dead zone form are applied to estimate the bound of estimation. By Lyapunov stability methods, we establish the stability criteria and prove the finite-time convergence of tracking errors. Finally, the simulations with 2-dof teleoperation system and comparisons with other control methods are performed, the effectuality and analysis of the proposed control method are shown.

This paper is organized as follows. In section II, the system dynamics, preliminaries of RBF neural network, and lemmas for controller design analysis are given. The adaptive finite-time controllers are designed and stability of closed-loop system is analyzed in section III. We illustrate some simulation results and analysis in section IV. Finally, this paper is concluded in section V.

There are some mathematical symbols used in this paper need to be explained as: \mathcal{R}^n is the $(n \times 1)$ -dimensional real vector space, for any vector $x \in \mathcal{R}^n$, the norm of x is represented as $\|x\|$. $\mathcal{R}^{n \times n}$ is the $(n \times n)$ -dimensional real matrix space. $\lambda_{\min}(A)$ and $\lambda_{\max}(A)$ denotes the minimum and maximum eigenvalues of the matrix A , for any matrix $A \in \mathcal{R}^{n \times n}$.

II. PRELIMINARY

A. DYNAMIC MODELS OF A TELEOPERATOR

The teleoperation system studied in this paper is consisted of a pair of single manipulators with the same mechanism at master and slave sides. Each n-dof manipulator is modeled by Euler-Lagrange theory. The dynamic descriptions of teleoperation system are expressed as:

$$\begin{cases} M_m(q_m)\ddot{q}_m + C_m(q_m, \dot{q}_m)\dot{q}_m + G_m(q_m) \\ \quad + F_m(q_m, \dot{q}_m) = \tau_m + J_m^T f_h, \\ M_s(q_s)\ddot{q}_s + C_s(q_s, \dot{q}_s)\dot{q}_s + G_s(q_s) \\ \quad + F_s(q_s, \dot{q}_s) = \tau_s - J_s^T f_e. \end{cases} \quad (1)$$

where m and s represent master side and slave side, respectively; $\ddot{q}_m \in \mathcal{R}^n$ and $\ddot{q}_s \in \mathcal{R}^n$ are the vectors of the joint accelerations; $\dot{q}_m \in \mathcal{R}^n$ and $\dot{q}_s \in \mathcal{R}^n$ denote the joint velocity vectors; $q_m \in \mathcal{R}^n$ and $q_s \in \mathcal{R}^n$ represent the vectors of the joint positions. $M_m(q_m) \in \mathcal{R}^{n \times n}$ and $M_s(q_s) \in \mathcal{R}^{n \times n}$ denote the inertia matrices; $C_m(q_m, \dot{q}_m) \in \mathcal{R}^{n \times n}$ and $C_s(q_s, \dot{q}_s) \in \mathcal{R}^{n \times n}$ are the matrices of centripetal and Coriolis torques; $G_m(q_m) \in \mathcal{R}^n$ and $G_s(q_s) \in \mathcal{R}^n$ denote the friction torque vectors; $\tau_m \in \mathcal{R}^n$ and $\tau_s \in \mathcal{R}^n$ represent the applied control torques; $f_h \in \mathcal{R}^n$ and $f_e \in \mathcal{R}^n$ describe the human-operator and environment forces applied to the manipulators at master and slave side; $J_m \in \mathcal{R}^{n \times n}$ and $J_s \in \mathcal{R}^{n \times n}$ denote the master and slave Jacobian matrices. The robotic manipulator in (1) has some well-known structure properties, for $i \in \{m, s\}$, the properties are revisited as following [30]:

Property 1: The inertia matrix $M_i(q_i)$ is the symmetric positive definite and has the upper and lower bounds as $0 < \lambda_{\min}(M_i(q_i))I \leq M_i(q_i) \leq \lambda_{\max}(M_i(q_i))I$, where I is an identity matrix.

Property 2: The $\dot{M}_i(q_i) - 2C_i(q_i, \dot{q}_i)$ is the skew symmetric matrix. Thus the equation $x^T(\dot{M}_i(q_i) - 2C_i(q_i, \dot{q}_i))x = 0$ for any vector $x \in \mathcal{R}^n$ is established.

Assumption 1: The human-operator force f_h , environment force f_e , master Jacobian matrix J_m , and slave Jacobian matrix J_s are all assumed to be locally essentially bounded.

In practical applications, it is very difficult to get the exact values of robot dynamic parameters. So uncertain dynamic parts are introduced into the description of master and slave robot models. For $j = m, s$, we have

$$\begin{aligned} M_i(q_i) &= M_{oi}(q_i) + \Delta M_i(q_i), \\ C_i(q_i, \dot{q}_i) &= C_{oi}(q_i, \dot{q}_i) + \Delta C_i(q_i, \dot{q}_i), \\ G_i(q_i) &= G_{oi}(q_i) + \Delta G_i(q_i). \end{aligned}$$

where $M_{oi}(q_i)$, $C_{oi}(q_i, \dot{q}_i)$, and $G_{oi}(q_i)$ represent the nominal parts in dynamic models; the matrices $\Delta M_i(q_i)$, $\Delta C_i(q_i, \dot{q}_i)$,

and vector $\Delta G_i(q_i)$ are the dynamic uncertain parts. Therefore, dynamic models of teleoperation system (1) can be rewritten as:

$$\begin{cases} M_{om}(q_m)\ddot{q}_m + C_{om}(q_m, \dot{q}_m)\dot{q}_m + G_{om}(q_m) \\ = \tau_m + J_m^T f_h + H_m(q_m, \dot{q}_m, \ddot{q}_m), \\ M_{os}(q_s)\ddot{q}_s + C_{os}(q_s, \dot{q}_s)\dot{q}_s + G_{os}(q_s) \\ = \tau_s - J_s^T f_e + H_s(q_s, \dot{q}_s, \ddot{q}_s). \end{cases} \quad (2)$$

where $H_m(q_m, \dot{q}_m, \ddot{q}_m)$ and $H_s(q_s, \dot{q}_s, \ddot{q}_s)$ are defined as:

$$\begin{cases} H_m(q_m, \dot{q}_m, \ddot{q}_m) = -\Delta M_m(q_m)\ddot{q}_m - \Delta C_m(q_m, \dot{q}_m)\dot{q}_m \\ - \Delta G_m(q_m) - F_m(q_m, \dot{q}_m), \\ H_s(q_s, \dot{q}_s, \ddot{q}_s) = -\Delta M_s(q_s)\ddot{q}_s - \Delta C_s(q_s, \dot{q}_s)\dot{q}_s \\ - \Delta G_s(q_s) - F_s(q_s, \dot{q}_s). \end{cases} \quad (3)$$

Remark 1: The uncertain parts $H_m(q_m, \dot{q}_m, \ddot{q}_m) \in \mathcal{R}^{n \times 1}$ and $H_s(q_s, \dot{q}_s, \ddot{q}_s) \in \mathcal{R}^{n \times 1}$ are upper bounded by the following form:

$$\|H_m(q_m, \dot{q}_m, \ddot{q}_m)\| \leq h_m, \|H_s(q_s, \dot{q}_s, \ddot{q}_s)\| \leq h_s. \quad (4)$$

B. RBF NEURAL NETWORKS

RBF neural network can approximate any smooth nonlinear function with arbitrary precision [31]. It has faster learning speed and can avoid the local minimum problem, which attracts the attention of researchers and applications on robot control [32]. The RBF neural network can approximate a continuous function $f(x) : \mathcal{R}^d \rightarrow \mathcal{R}^e$, which can be described as:

$$f(x) = w^T \varphi(x) + \varepsilon. \quad (5)$$

where $\varphi(x) = [\varphi_1, \varphi_2, \dots, \varphi_n]^T$ denotes the output vector of the hidden layer, each element $\varphi_i(x)$ can be expressed as:

$$\varphi_i(x) = \exp\left[-\|x - c_i\|^2 / (2b_i)\right], \quad i = 1, 2, \dots, n. \quad (6)$$

$x \in A_x \subset \mathcal{R}^d$ is the input data vector; $w \in \mathcal{R}^{n \times e}$ is the weight matrix to connect with hidden layer and output; $c_i \in \mathcal{R}^d$ and $b_i > 0$ are the center and width of the i -th node in hidden neuron; $\varepsilon \in \mathcal{R}^e$ is the approximation error of RBF neural network.

Remark 2: According to the universal approximation property of neural networks, the uncertain part of $H_m(q_m, \dot{q}_m, \ddot{q}_m)$ and $H_s(q_s, \dot{q}_s, \ddot{q}_s)$ in (3) can be described by the RBF neural networks as:

$$\begin{cases} H_m(q_m, \dot{q}_m, \ddot{q}_m) = W_m^T \varphi_m + \varepsilon_m, \\ H_s(q_s, \dot{q}_s, \ddot{q}_s) = W_s^T \varphi_s + \varepsilon_s. \end{cases} \quad (7)$$

$W_m^T, W_s^T, \varepsilon_m$, and ε_s are the ideal weights in approximation, respectively. The approximation errors ε_m and ε_s have the upper bounds as $\|\varepsilon_m\| \leq \bar{\varepsilon}_m, \|\varepsilon_s\| \leq \bar{\varepsilon}_s$.

Thus the dynamic models (2) can be written as:

$$\begin{cases} M_{om}(q_m)\ddot{q}_m + C_{om}(q_m, \dot{q}_m)\dot{q}_m + G_{om}(q_m) \\ = \tau_m + J_m^T f_h + W_m^T \varphi_m + \varepsilon_m, \\ M_{os}(q_s)\ddot{q}_s + C_{os}(q_s, \dot{q}_s)\dot{q}_s + G_{os}(q_s) \\ = \tau_s - J_s^T f_e + W_s^T \varphi_s + \varepsilon_s. \end{cases} \quad (8)$$

Remark 3: As the assumption 1, human-operator torque $J_m^T f_h$ and environment torque $J_s^T f_e$ have upper bounds which can be described as

$$\|\varepsilon_m + J_m^T f_h\| \leq \omega_m, \quad \|\varepsilon_s - J_s^T f_e\| \leq \omega_s. \quad (9)$$

C. THE LEMMAS USED IN THIS PAPER

In this paper, some lemmas [33] are applied to analyze the control system:

Lemma 1: Assume if $a > 0, b > 0$, and $0 < c < 1$, then the following inequality holds:

$$(a + b)^c \leq a^c + b^c.$$

Lemma 2: Considering a dynamic system as: $\dot{x} = f(x)$, initial state: $f(0) = 0, x \in \mathcal{R}^n$. This system is finite-time stable, if there exists a positive scalar function $V(x)$, values a, b , and c , satisfy $a, b > 0, 0 < c < 1$, and following inequality holds:

$$\dot{V}(x) \leq -aV(x) - bV^c(x).$$

and the setting time can be calculated as

$$T \leq \frac{1}{a(1-c)} \ln \frac{aV^{1-c}(x_0) + b}{b}.$$

III. CONTROLLER DESIGN

In this section, the adaptive finite-time control based on a novel NTSM is proposed for teleoperation system with time-variable delays and dynamic uncertainties. First, the integral term of synchronization error is introduced to define the new terminal sliding mode surface. The RBF neural networks are employed to approximate the dynamic uncertain parts of $H_m(q_m, \dot{q}_m, \ddot{q}_m)$ and $H_s(q_s, \dot{q}_s, \ddot{q}_s)$ in (2). The adaptive laws are designed to converge synchronization tracking errors to zero in finite-time. Then, the stability of closed-loop teleoperation system is proved via the Lyapunov stability theorem.

A. ADAPTIVE FINITE-TIME CONTROLLER DESIGN

We define the coordination joint tracking errors e_m, e_s between master robot and slave robot is:

$$\begin{aligned} e_m(t) &= q_m(t) - q_s(t - d_s), \\ e_s(t) &= q_s(t) - q_m(t - d_m). \end{aligned} \quad (10)$$

where the d_m and d_s are the time-varying communication delays between master and slave sides.

Assumption 2: The time-varying delays d_m and d_s are assumed to have the upper and lower bound and satisfy: $0 < d_i < D_i, |\dot{d}_i| \leq \bar{D}_i$, and $|\ddot{d}_i| \leq \bar{\ddot{D}}_i$ for $i = m, s$.

The control object is that the position tracking errors e_m and e_s can converge to a small neighborhood of zero under asymmetric time-varying communication delays and dynamic uncertainties, whether existing operator or environment forces in the teleoperation system.

The velocity errors \dot{e}_m, \dot{e}_s and acceleration errors \ddot{e}_m, \ddot{e}_s can also be defined as following:

$$\dot{e}_m(t) = \dot{q}_m(t) - \dot{q}_s(t - d_s)(1 - \dot{d}_s),$$

$$\begin{aligned} \dot{e}_s(t) &= \dot{q}_s(t) - \dot{q}_m(t - d_m)(1 - \dot{d}_m), \\ \ddot{e}_m(t) &= \ddot{q}_m(t) - \ddot{q}_s(t - d_s)(1 - \dot{d}_s)^2 \\ &\quad + \dot{q}_s(t - d_s)\ddot{d}_s, \\ \ddot{e}_s(t) &= \ddot{q}_s(t) - \ddot{q}_m(t - d_m)(1 - \dot{d}_m)^2 \\ &\quad + \dot{q}_m(t - d_m)\ddot{d}_m. \end{aligned} \quad (11)$$

The nonsingular TSMs used in this work are defined as:

$$\begin{aligned} s_m &= \dot{e}_m + \lambda_m e_m + \zeta_m(e_m), \\ s_s &= \dot{e}_s + \lambda_s e_s + \zeta_s(e_s). \end{aligned} \quad (12)$$

where for $i = m, s$, function $\zeta_i(e_i) = \alpha_i \text{sig}(e_i)^{r_{i1}} + \beta_i \int_0^1 \text{sig}(e_i)^{r_{i2}} d\tau$. Parameters of $\alpha_i = \text{diag}(\alpha_{i1}, \dots, \alpha_{in})$, $\beta_i = \text{diag}(\beta_{i1}, \dots, \beta_{in})$, and $\lambda_i = \text{diag}(\lambda_{i1}, \dots, \lambda_{in})$ are all positive-definite diagonal matrices, $1 < r_{i1} < 2$, $0 < r_{i2} < 1$. The function $\text{sig}(x)^r$ is defined as: $\text{sig}(x)^r = [|x_1|^r \text{sign}(x_1), |x_2|^r \text{sign}(x_2), \dots, |x_n|^r \text{sign}(x_n)]^T$, for vector $x = [x_1, x_2, \dots, x_n]^T \in \mathcal{R}^n$.

Remark 4: The sliding mode surface (12) contains the integral term of tracking error, compared with the conventional PD-type sliding surfaces, (12) can provide more stable response and better dynamic characteristics.

Based on the differential definition of $\text{sig}(x)^r$ [22], the differential of (12) to time is:

$$\begin{aligned} \dot{s}_m &= \ddot{e}_m + \lambda_m \dot{e}_m + \dot{\zeta}_m(e_m), \\ \dot{s}_s &= \ddot{e}_s + \lambda_s \dot{e}_s + \dot{\zeta}_s(e_s). \end{aligned} \quad (13)$$

where $\dot{\zeta}_m(e_m) = \alpha_m r_{m1} \text{diag}(|e_m|)^{r_{m1}-1} \dot{e}_m + \beta_m \text{sig}(e_m)^{r_{m2}}$, $\dot{\zeta}_s(e_s) = \alpha_s r_{s1} \text{diag}(|e_s|)^{r_{s1}-1} \dot{e}_s + \beta_s \text{sig}(e_s)^{r_{s2}}$.

The proposed controllers are designed as follows:

$$\begin{aligned} \tau_m &= \tau_{m1} + \tau_{m2} + \tau_{m3}, \\ \tau_s &= \tau_{s1} + \tau_{s2} + \tau_{s3}. \end{aligned} \quad (14)$$

The τ_{m1} and τ_{s1} are given as

$$\begin{aligned} \tau_{m1} &= M_{om}[\ddot{q}_s(t - d_s)(1 - \dot{d}_s)^2 - \dot{q}_s(t - d_s)\ddot{d}_s \\ &\quad - \lambda_m \dot{e}_m - \alpha_m r_{m1} \text{diag}(|e_m|)^{r_{m1}-1} \dot{e}_m \\ &\quad - \beta_m \text{sig}(e_m)^{r_{m2}}] + C_{om}(\dot{q}_m - s_m) + G_{om}, \\ \tau_{s1} &= M_{os}[\ddot{q}_m(t - d_m)(1 - \dot{d}_m)^2 - \dot{q}_m(t - d_m)\ddot{d}_m \\ &\quad - \lambda_s \dot{e}_s - \alpha_s r_{s1} \text{diag}(|e_s|)^{r_{s1}-1} \dot{e}_s \\ &\quad - \beta_s \text{sig}(e_s)^{r_{s2}}] + C_{os}(\dot{q}_s - s_s) + G_{os}. \end{aligned} \quad (15)$$

The τ_{m2} and τ_{s2} are given as

$$\begin{aligned} \tau_{m2} &= -K_{m1}s_m - K_{m2}\text{sig}(s_m)^\sigma, \\ \tau_{s2} &= -K_{s1}s_s - K_{s2}\text{sig}(s_s)^\sigma. \end{aligned} \quad (16)$$

where $K_{m1} = \text{diag}(k_{m11}, \dots, k_{m1n})$, $K_{m2} = \text{diag}(k_{m21}, \dots, k_{m2n})$, $K_{s1} = \text{diag}(k_{s11}, \dots, k_{s1n})$, and $K_{s2} = \text{diag}(k_{s21}, \dots, k_{s2n})$ are all positive diagonal matrices, and $0 < \sigma < 1$.

Considering the approximation and upper bound of uncertain parts in the system, for $i = m, s$ the third term of controllers τ_{m3} and τ_{s3} are described as:

$$\tau_{i3} = \begin{cases} -\hat{W}_i^T \varphi_i - (\hat{\omega}_i + \eta_i) \frac{s_i}{\|s_i\|}, & \text{if } \|s_i\| \neq 0 \\ -\hat{W}_i^T \varphi_i, & \text{if } \|s_i\| = 0. \end{cases} \quad (17)$$

where $\hat{\omega}_i$ is the upper bounds estimation of adaptive parameters, η_i is the positive controller design parameters.

The adaptive tuning laws are designed in following terms:

$$\dot{\hat{W}}_i = \Gamma_i \varphi_i s_i^T. \quad (18)$$

$$\dot{\hat{\omega}}_i = \xi_i \|s_i\|. \quad (19)$$

where $i = m, s$, Γ_i and ξ_i are the positive constants.

Remark 5: In practical control, as the uncertain parameters and communication delays with time-varying, $\|s_m\|$ and $\|s_s\|$ cannot exactly reach to the zero in finite-time, the adaptive parameters $\hat{\omega}_m$ and $\hat{\omega}_s$ could be increased boundlessly [23]. The way to solve this problem is to improve the adaptive turning law (19) as the dead zoom form:

$$\dot{\hat{\omega}}_i = \begin{cases} \xi_i \|s_i\|, & \text{if } \|s_i\| \geq \mu_i \\ 0, & \text{if } \|s_i\| < \mu_i, \end{cases} \quad i = m, s. \quad (20)$$

where μ_i is the small positive constant.

B. STABILITY ANALYSIS

Theory 1. Considering the teleoperation system (1) with the control laws in (14)-(17) and adaptive laws in (18) (20), the closed-loop teleoperation system is stable and the states can converge to zero as $\|s_m\| = 0$ and $\|s_s\| = 0$ in finite-time, if the inequality of $\eta_m \geq |\tilde{\omega}_m| + \|\tilde{W}_m^T \varphi_m\|$ and $\eta_s \geq |\tilde{\omega}_s| + \|\tilde{W}_s^T \varphi_s\|$ are established. Where $\tilde{W}_i = W_i - \hat{W}_i$, $\tilde{\omega}_i = \omega_i - \hat{\omega}_i$ for $i = m, s$.

Proof: 1) Let us consider the Lyapunov candidate V for system stability analysis as:

$$\begin{aligned} V &= \frac{1}{2} s_m^T M_{om} s_m + \frac{1}{2} \text{tr}(\tilde{W}_m^T \Gamma_m^{-1} \tilde{W}_m) + \frac{1}{2} \xi_m^{-1} \tilde{\omega}_m^2 \\ &\quad + \frac{1}{2} s_s^T M_{os} s_s + \frac{1}{2} \text{tr}(\tilde{W}_s^T \Gamma_s^{-1} \tilde{W}_s) + \frac{1}{2} \xi_s^{-1} \tilde{\omega}_s^2. \end{aligned} \quad (21)$$

With the Property 2, dynamics in (8), acceleration errors \ddot{e}_m, \ddot{e}_s in (11), and the differential of \dot{s}_m and \dot{s}_s in (13), the differential of function V is given as follow:

$$\begin{aligned} \dot{V} &= s_m^T \{ \tau_m + W_m^T \varphi_m + \varepsilon_m + J_m^T f_h - C_{om} \dot{q}_m - G_{om} \\ &\quad + C_{om} s_m + M_{om} [-\ddot{q}_s(t - d_s)(1 - \dot{d}_s)^2 + \dot{q}_s(t - d_s)\ddot{d}_s \\ &\quad + \lambda_m \dot{e}_m + \dot{\zeta}_m] \} + s_s^T \{ \tau_s + W_s^T \varphi_s + \varepsilon_s - J_s^T f_e - C_{os} \dot{q}_s \\ &\quad - G_{os} + C_{os} s_s + M_{os} [-\ddot{q}_m(t - d_m)(1 - \dot{d}_m)^2 \\ &\quad + \dot{q}_m(t - d_m)\ddot{d}_m + \lambda_s \dot{e}_s + \dot{\zeta}_s] \} - \text{tr}(\tilde{W}_m^T \Gamma_m^{-1} \dot{\hat{W}}_m) \\ &\quad - \xi_m^{-1} \tilde{\omega}_m \dot{\hat{\omega}}_m - \text{tr}(\tilde{W}_s^T \Gamma_s^{-1} \dot{\hat{W}}_s) - \xi_s^{-1} \tilde{\omega}_s \dot{\hat{\omega}}_s. \end{aligned} \quad (22)$$

Employing the control laws (14)-(16) we can get

$$\begin{aligned} \dot{V} &= s_m^T [\tau_{m3} + W_m^T \varphi_m + \varepsilon_m + J_m^T f_h - K_{m1} s_m - K_{m2} \text{sig}(s_m)^\sigma] \\ &\quad + s_s^T [\tau_{s3} + W_s^T \varphi_s + \varepsilon_s - J_s^T f_e - K_{s1} s_s - K_{s2} \text{sig}(s_s)^\sigma] \\ &\quad - \text{tr}(\tilde{W}_m^T \Gamma_m^{-1} \dot{\hat{W}}_m) - \xi_m^{-1} \tilde{\omega}_m \dot{\hat{\omega}}_m \\ &\quad - \text{tr}(\tilde{W}_s^T \Gamma_s^{-1} \dot{\hat{W}}_s) - \xi_s^{-1} \tilde{\omega}_s \dot{\hat{\omega}}_s. \end{aligned} \quad (23)$$

If $\|s_m\| \geq \mu_m$ and $\|s_s\| \geq \mu_s$, with (9), the control laws (17), adaptive laws (18), (20), and for vectors $x, y \in \mathcal{R}^n$, $x^T y \leq |x^T y| \leq \|x\| \|y\|$, we can get

$$\dot{V} = -[s_m^T K_{m1} s_m + s_m^T K_{m2} \text{sig}(s_m)^\sigma + s_s^T K_{s1} s_s + s_s^T K_{s2} \text{sig}(s_s)^\sigma]$$

$$\begin{aligned}
 & + s_m^T(\varepsilon_m + J_m^T f_h) - (\hat{\omega}_m + \eta_m)\|s_m\| - \tilde{\omega}_m\|s_m\| \\
 & + s_s^T(\varepsilon_s - J_s^T f_e) - (\hat{\omega}_s + \eta_s)\|s_s\| - \tilde{\omega}_s\|s_s\| \\
 \leq & -[s_m^T K_{m1} s_m + s_m^T K_{m2} \text{sig}(s_m)^\sigma + s_s^T K_{s1} s_s + s_s^T K_{s2} \text{sig}(s_s)^\sigma] \\
 & + \omega_m\|s_m\| - (\hat{\omega}_m + \eta_m)\|s_m\| \\
 & - \tilde{\omega}_m\|s_m\| + \omega_s\|s_s\| - (\hat{\omega}_s + \eta_s)\|s_s\| - \tilde{\omega}_s\|s_s\| \\
 = & -[s_m^T K_{m1} s_m + s_m^T K_{m2} \text{sig}(s_m)^\sigma + s_s^T K_{s1} s_s + s_s^T K_{s2} \text{sig}(s_s)^\sigma] \\
 & - \eta_m\|s_m\| - \eta_s\|s_s\| < 0. \tag{24}
 \end{aligned}$$

It follows that if $\|s_m\| \leq \mu_m$ and $\|s_s\| \leq \mu_s$, with (9), the control laws (17), adaptive laws (18), and (20) we have

$$\begin{aligned}
 \dot{V} \leq & -[s_m^T K_{m1} s_m + s_m^T K_{m2} \text{sig}(s_m)^\sigma + s_s^T K_{s1} s_s \\
 & + s_s^T K_{s2} \text{sig}(s_s)^\sigma] + \omega_m\|s_m\| - (\hat{\omega}_m + \eta_m)\|s_m\| \\
 & + \omega_s\|s_s\| - (\hat{\omega}_s + \eta_s)\|s_s\| \\
 = & -[s_m^T K_{m1} s_m + s_m^T K_{m2} \text{sig}(s_m)^\sigma + s_s^T K_{s1} s_s \\
 & + s_s^T K_{s2} \text{sig}(s_s)^\sigma] + (\tilde{\omega}_m - \eta_m)\|s_m\| \\
 & + (\tilde{\omega}_s - \eta_s)\|s_s\|. \tag{25}
 \end{aligned}$$

If $\eta_m \geq |\tilde{\omega}_m| + \|W_m^T \varphi_m\|$, $\eta_s \geq |\tilde{\omega}_s| + \|W_s^T \varphi_s\|$, we can obtain

$$\begin{aligned}
 \dot{V} \leq & -s_m^T K_{m1} s_m - s_m^T K_{m2} \text{sig}(s_m)^\sigma - s_s^T K_{s1} s_s \\
 & - s_s^T K_{s2} \text{sig}(s_s)^\sigma \leq 0. \tag{26}
 \end{aligned}$$

Similarly, whether $\|s_m\| \leq \mu_m$ or $\|s_s\| \leq \mu_s$, with (9), the $\dot{V} \leq 0$ is always hold. Therefore, the stability of closed-loop control system has been verified.

2) The finite-time proof is described as following. We define another Lyapunov function candidate:

$$U = \frac{1}{2} s_m^T M_{om} s_m + \frac{1}{2} s_s^T M_{os} s_s. \tag{27}$$

Applying the (8), (9), (11), (13), the control laws in (14)-(17), adaptive laws (18), (20), we have

$$\begin{aligned}
 \dot{U} \leq & -[s_m^T K_{m1} s_m + s_m^T K_{m2} \text{sig}(s_m)^\sigma + s_s^T K_{s1} s_s \\
 & + s_s^T K_{s2} \text{sig}(s_s)^\sigma] + \|s_m\| \|\tilde{W}_m^T \varphi_m\| + \|s_s\| \|\tilde{W}_s^T \varphi_s\| \\
 & + \omega_m\|s_m\| - (\hat{\omega}_m + \eta_m)\|s_m\| \\
 & + \omega_s\|s_s\| - (\hat{\omega}_s + \eta_s)\|s_s\| \\
 \leq & -[s_m^T K_{m1} s_m + s_m^T K_{m2} \text{sig}(s_m)^\sigma + s_s^T K_{s1} s_s \\
 & + s_s^T K_{s2} \text{sig}(s_s)^\sigma] + (|\tilde{\omega}_m| + \|\tilde{W}_m^T \varphi_m\| - \eta_m)\|s_m\| \\
 & + (|\tilde{\omega}_s| + \|\tilde{W}_s^T \varphi_s\| - \eta_s)\|s_s\|. \tag{28}
 \end{aligned}$$

As $\eta_m \geq |\tilde{\omega}_m| + \|\tilde{W}_m^T \varphi_m\|$, $\eta_s \geq |\tilde{\omega}_s| + \|\tilde{W}_s^T \varphi_s\|$, we can obtain

$$\begin{aligned}
 \dot{U} \leq & -s_m^T K_{m1} s_m - s_m^T K_{m2} \text{sig}(s_m)^\sigma \\
 & - s_s^T K_{s1} s_s - s_s^T K_{s2} \text{sig}(s_s)^\sigma \\
 = & -s_m^T K_{m1} M_{om}^{-1} M_{om} s_m - s_m^T K_{m2} \text{sig}(s_m)^\sigma \\
 & - s_s^T K_{s1} M_{os}^{-1} M_{os} s_s - s_s^T K_{s2} \text{sig}(s_s)^\sigma. \tag{29}
 \end{aligned}$$

$K_{m1} M_{om}^{-1}$, $K_{m2} M_{om}^{-\frac{\sigma+1}{2}}$, $K_{s1} M_{os}^{-1}$, and $K_{s2} M_{os}^{-\frac{\sigma+1}{2}}$ are the diagonal matrices. We define

$$k_{m1} = \lambda_{\min}(K_{m1} M_{om}^{-1}) = \frac{\lambda_{\min}(K_{m1})}{\lambda_{\min}(M_{om}^{-1})} > 0,$$

$$k_{s1} = \lambda_{\min}(K_{s1} M_{os}^{-1}) = \frac{\lambda_{\min}(K_{s1})}{\lambda_{\min}(M_{os}^{-1})} > 0.$$

According to the meaning of diagonal matrix and lemma 1, we can write (29) as following relational expression:

$$\begin{aligned}
 \dot{U} \leq & -k_{m1} s_m^T M_{om} s_m - \lambda_{\min}(K_{m2})(s_m^T s_m)^{\frac{\sigma+1}{2}} \\
 & - k_{s1} s_s^T M_{os} s_s - \lambda_{\min}(K_{s2})(s_s^T s_s)^{\frac{\sigma+1}{2}} \\
 \leq & -k_{m1} s_m^T M_{om} s_m - \lambda_{\min}(K_{m2})(s_m^T M_{om}^{-1} M_{om} s_m)^{\frac{\sigma+1}{2}} \\
 & - k_{s1} s_s^T M_{os} s_s - \lambda_{\min}(K_{s2})(s_s^T M_{os}^{-1} M_{os} s_s)^{\frac{\sigma+1}{2}}. \tag{30}
 \end{aligned}$$

We define

$$k_{m2} = \lambda_{\min}(K_{m2}) \lambda_{\min}(M_{om}^{-\frac{\sigma+1}{2}}) > 0,$$

$$k_{s2} = \lambda_{\min}(K_{s2}) \lambda_{\min}(M_{os}^{-\frac{\sigma+1}{2}}) > 0.$$

The (30) can be written as

$$\begin{aligned}
 \dot{U} \leq & -2k_{m1}(\frac{1}{2} s_m^T M_{om} s_m) - 2k_{s1}(\frac{1}{2} s_s^T M_{os} s_s) \\
 & - 2^{\frac{\sigma+1}{2}} k_{m2}(\frac{1}{2} s_m^T M_{om} s_m)^{\frac{\sigma+1}{2}} \\
 & - 2^{\frac{\sigma+1}{2}} k_{s2}(\frac{1}{2} s_s^T M_{os} s_s)^{\frac{\sigma+1}{2}} \\
 \leq & -k_1 U - k_2 U^{\frac{\sigma+1}{2}}. \tag{31}
 \end{aligned}$$

where $\rho = \frac{\sigma+1}{2}$, $k_1 = \min(2k_{m1}, 2k_{s1})$, and $k_2 = \min(2^{\frac{\sigma+1}{2}} k_{m2}, 2^{\frac{\sigma+1}{2}} k_{s2})$. So based on the lemma 2, the trajectory errors at master and slave sides can converge to zero in finite time. The reaching time can be calculated as

$$T \leq \frac{1}{k_1(1-\rho)} \ln \frac{k_1 U^{1-\rho}(0) + k_2}{k_2}. \tag{32}$$

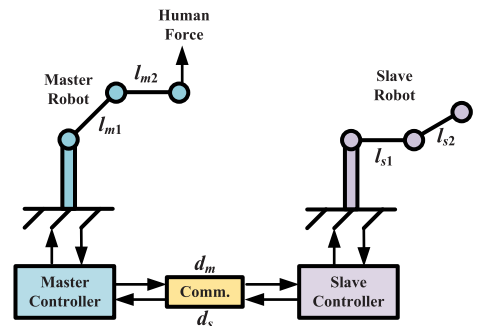


FIGURE 1. Teleoperation system simulation considered in simulation analysis.

IV. SIMULATIONS

This section describes the simulation experiments to evaluate the proposed control scheme. We used MATLAB software to perform related simulation experiments. The master and slave robots in teleoperation system are considered to be the 2-dof robot arms with revolute joints. The system structure is shown in Fig. 1, the d_m and d_s represent the communication delays between master and slave controllers. We define $z_{i1} = (m_{i1} + m_{i2})l_{i1}^2$, $z_{i2} = m_{i2}l_{i2}^2$, $z_{i3} = 2m_{i2}l_{i1}l_{i2}$, $z_{i4} = (m_{i1} + m_{i2})l_{i1}$,

and $z_{i5} = m_{i2}l_{i2}$ for $i = m, s$. The dynamic descriptions of teleoperation system are given as following:

$$M_{oi}(q_i) = \begin{bmatrix} z_{i1} + z_{i2} + 2z_{i3}\cos q_{i2} & z_{i2} + z_{i3}\cos q_{i2} \\ z_{i2} + z_{i3}\cos q_{i2} & z_{i2} \end{bmatrix},$$

$$C_{oi}(q_i, \dot{q}_i) = \begin{bmatrix} -z_{i3}\dot{q}_{i2}\sin q_{i2} & -z_{i3}(\dot{q}_{i1} + \dot{q}_{i2})\sin q_{i2} \\ z_{i3}\dot{q}_{i1}\sin q_{i2} & 0 \end{bmatrix},$$

$$G_{oi}(q_i) = [G_{oi1} \quad G_{oi2}]^T,$$

$$F_i(q_i, \dot{q}_i) = f_{i1}q_i + f_{i2}\text{sign}(\dot{q}_i),$$

$$J_i = \begin{bmatrix} J_{i11} & J_{i12} \\ J_{i21} & J_{i22} \end{bmatrix},$$

$$G_{oi1} = -z_{i4}g\cos q_{i1} + z_{i5}\cos(q_{i1} + q_{i2}),$$

$$G_{oi2} = z_{i5}\cos(q_{i1} + q_{i2}),$$

$$J_{i11} = -l_{i1}\sin(q_{i1}) - l_{i2}\sin(q_{i1} + q_{i2}),$$

$$J_{i12} = -l_{i2}\sin(q_{i1} + q_{i2}),$$

$$J_{i21} = l_{i1}\cos(q_{i1}) + l_{i2}\cos(q_{i1} + q_{i2}),$$

$$J_{i22} = l_{i2}\cos(q_{i1} + q_{i2}).$$

For simulation analysis, we choose the parameters in teleoperation dynamic as [34]: $m_{i1} = 2.51\text{kg}$, $m_{i2} = 1.32\text{kg}$, $l_{i1} = 0.87\text{m}$, $l_{i2} = 0.76\text{m}$, $f_{m1} = 0.3$, $f_{m2} = 0.2$, $f_{s1} = 0.2$, $f_{s2} = 0.1$, $g = 9.8\text{m/s}^2$. The values of z_{i1} , z_{i2} , z_{i3} , z_{i4} , and z_{i5} can be calculated by the above parameters, however, in practical we can only obtain inaccurate parameters of dynamic models, so we use the values of $z_{i1} = 2.5$, $z_{i2} = 0.7$, $z_{i3} = 0.8$, $z_{i4} = 3.0$, and $z_{i5} = 0.8$ as the nominal model parameters for controllers design; the uncertain parts are described as: $\Delta M_m(q_m) = 0.1\sin(2t)M_{om}(q_m)$, $\Delta C_m(q_m, \dot{q}_m) = 0.08\sin(3t)C_{om}(q_m, \dot{q}_m)$, $\Delta G_m(q_m) = 0.05\sin(3t)G_{om}(q_m)$, $\Delta M_s(q_s) = 0.1\sin(2t)M_{os}(q_s)$, $\Delta C_s(q_s, \dot{q}_s) = 0.1\sin(4t)C_{os}(q_s, \dot{q}_s)$, $\Delta G_s(q_s) = 0.06\sin(4t)G_{os}(q_s)$. The initial states of system are set as $q_m(0) = [0.1, 0.15]^T$, $\dot{q}_m(0) = [0, 0]^T$, $q_s(0) = [0, 0]^T$, $\dot{q}_s(0) = [0, 0]^T$. The parameters of controllers are $\lambda_m = \text{diag}(6.6, 6.1)$, $\lambda_s = \text{diag}(8.5, 7.9)$, $\alpha_m = \text{diag}(11.5, 11.8)$, $\alpha_s = \text{diag}(9.5, 9.3)$, $\beta_m = \text{diag}(5.15, 3.15)$, $\beta_s = \text{diag}(3.15, 3.35)$, $r_{m1} = 1.2$, $r_{m2} = 0.48$, $r_{s1} = 1.3$, $r_{s2} = 0.5$, $K_{m1} = \text{diag}(11.8, 11.2)$, $K_{m2} = \text{diag}(8.0, 7.8)$, $K_{s1} = \text{diag}(12.5, 12.1)$, $K_{s2} = \text{diag}(8.3, 7.8)$, $\sigma = 0.12$, $\Gamma_m = 17.8$, $\Gamma_s = 15.8$, $\mu_m = 0.05$, $\mu_s = 0.05$, $\xi_m = 1.1$, $\xi_s = 0.8$. The time-varying delays at master and slave sides are set as $d_m = 0.2 + 0.05\sin(t) + 0.06\sin(3t) + 0.02\sin(6t)$ and $d_s = 0.2 + 0.05\sin(t) + 0.06\sin(3t) + 0.02\sin(8t)$ in Fig. 2. We assumed that the human operator force exerts at y direction as shown in Fig. 3, and no force is exerted in x direction. The force applied from 10 s to 12 s and 20 s to 22 s are 30N and 40N respectively. The slave robot is in the free state with no external force.

We implement two parts of simulation experiments in this section to show the performance of proposed control method: the first part is synchronization tracking control analysis of teleoperation with varying time delays, dynamic uncertainties, and the human-operator force effect; the second part is the comparisons with other synchronization control methods under the same experimental conditions as above part.

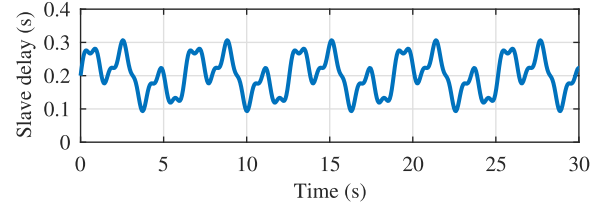
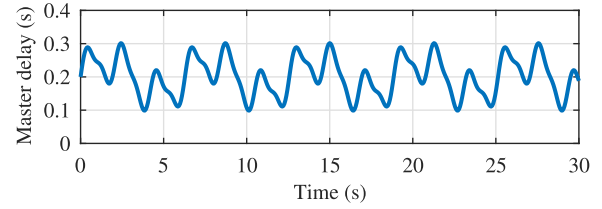


FIGURE 2. Communication delays at master side d_m and slave side d_s .

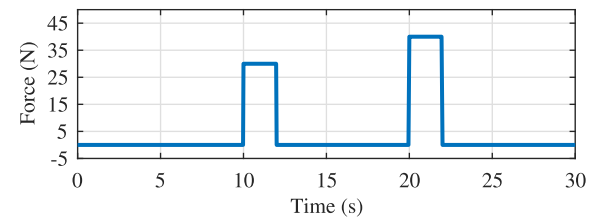


FIGURE 3. External force of the human operator f_h in y direction.

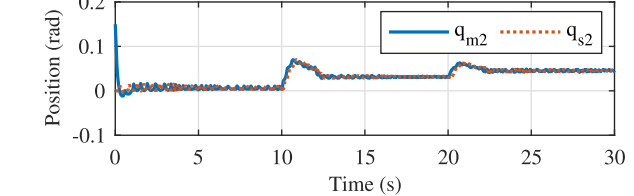
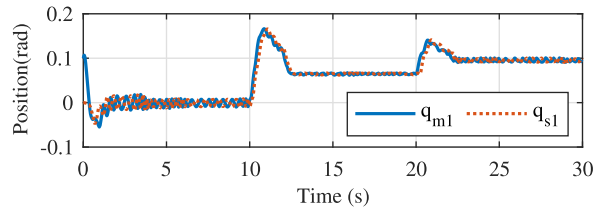


FIGURE 4. Joint positions of master and slave robots q_{m1} , q_{m2} , q_{s1} , and q_{s2} .

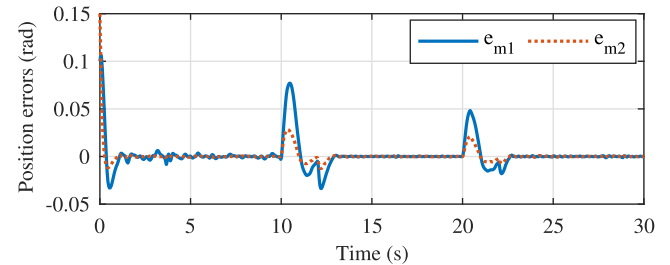


FIGURE 5. Synchronization position errors at the master side e_{m1} and e_{m2} .

The simulation results for proposed control, PD1 and PD2 are shown in Fig. 12 and Fig. 13, respectively. From which, it can be seen that the proposed NTSM produces a better tracking performance over PD control in [31] and [35].

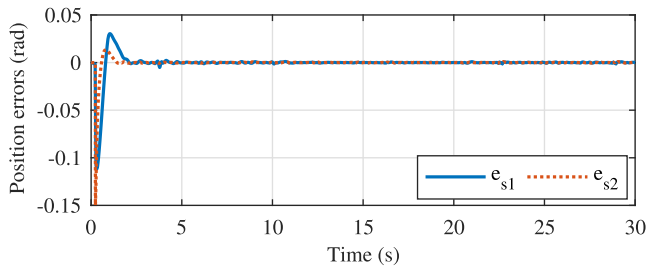


FIGURE 6. Synchronization position errors at the slave side e_{s1} and e_{s2} .

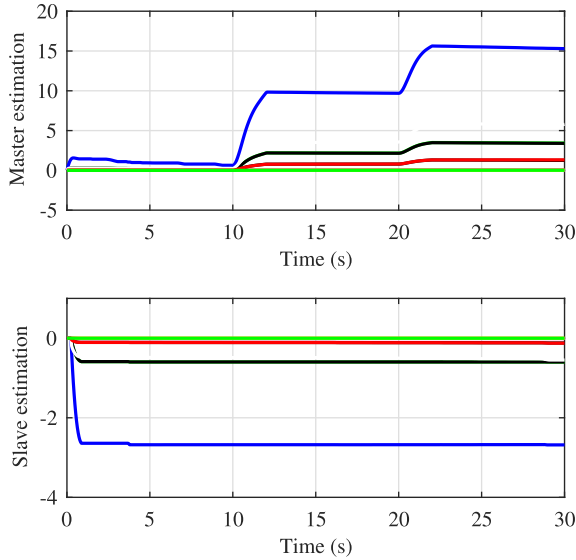


FIGURE 7. Adaptive estimated parameters \hat{W}_m and \hat{W}_s of uncertain parts .

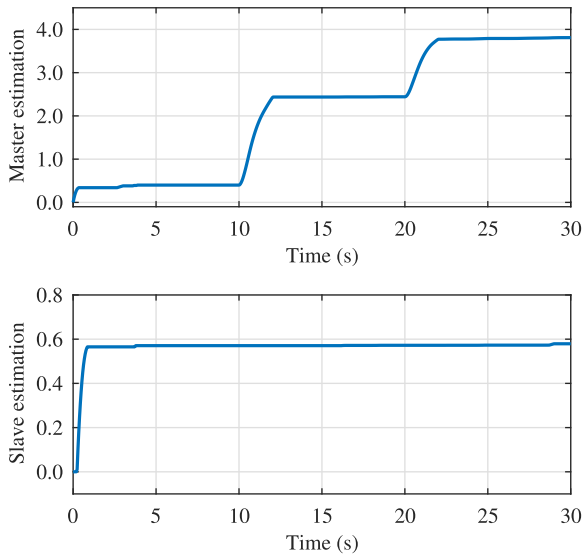


FIGURE 8. Adaptive estimated values $\hat{\omega}_m$ and $\hat{\omega}_s$ of upper bounds .

A. PERFORMANCE ANALYSIS OF PROPOSED CONTROLLERS

The simulation results of master and slave robots joint positions are shown in Fig. 4. The synchronization tracking errors e_{m1} , e_{m2} at master side and the tracking errors e_{s1} , e_{s2} at slave side are shown in Fig. 5 and Fig. 6, respectively. It is obvious

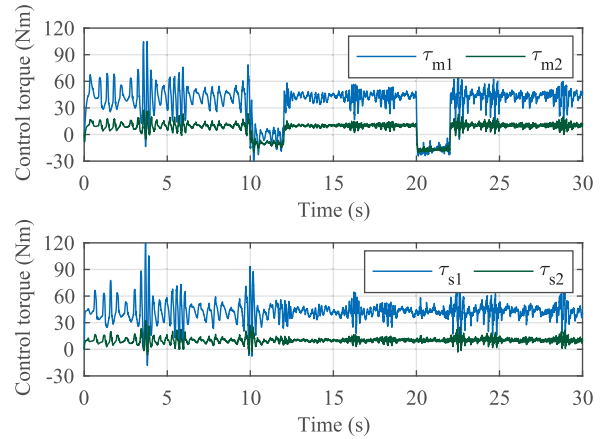


FIGURE 9. Master control torque τ_m and slave control torque τ_s .

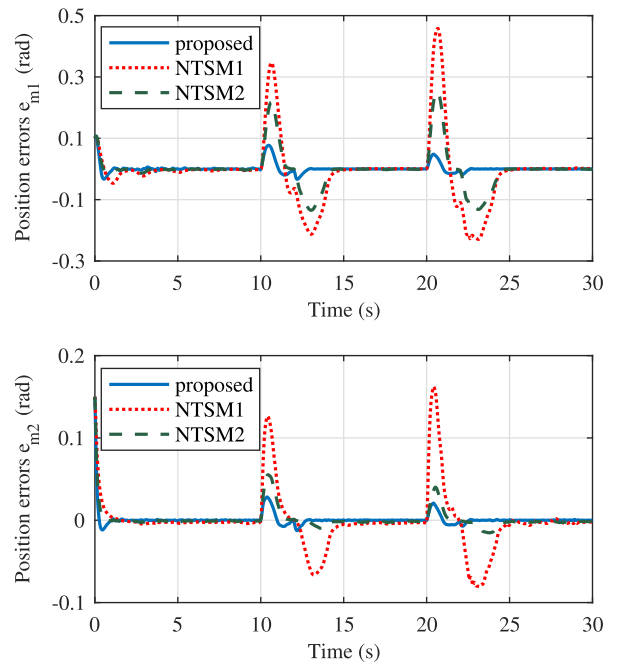


FIGURE 10. Tracking error comparison with other NTSM methods at master side.

that the synchronization tracking errors can converge to zero in finite time with operator force and varying time delays. The adaptive estimated values \hat{W}_m , \hat{W}_s , $\hat{\omega}_m$, and $\hat{\omega}_s$ are given in Fig. 7 and Fig. 8. It can be obtained that the adaptive values are bounded, which infer that the approximation errors of RBF neural networks are bounded and the closed loop system can stay in stable state. The control torques of master and slave robots are shown in Fig. 9. The effect of time-varying delays and sign functions cause the oscillations in control torque signals. Our simulation experiments show that the oscillatory degree of control torque is inversely proportional to the speed of system regulation.

B. COMPARISON WITH OTHER CONTROL SCHEME

To elucidate the effectiveness of proposed control method, the comparisons of control effect with NFTSM in [25]

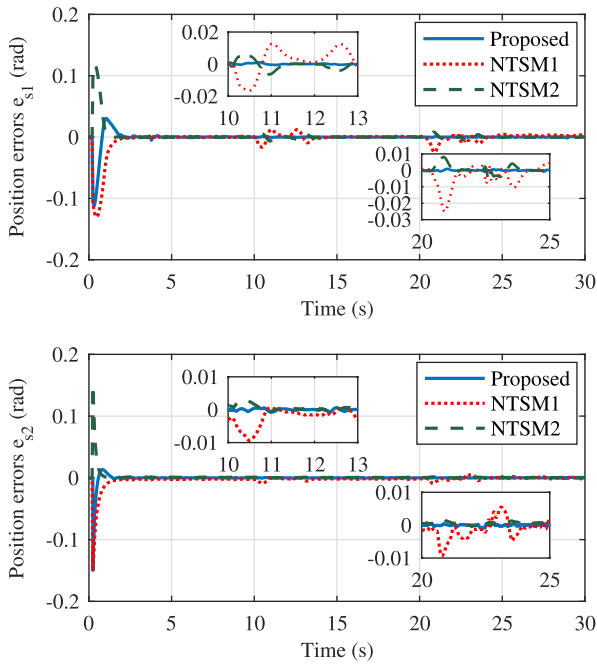


FIGURE 11. Tracking error comparison with other NTSM methods at slave side.

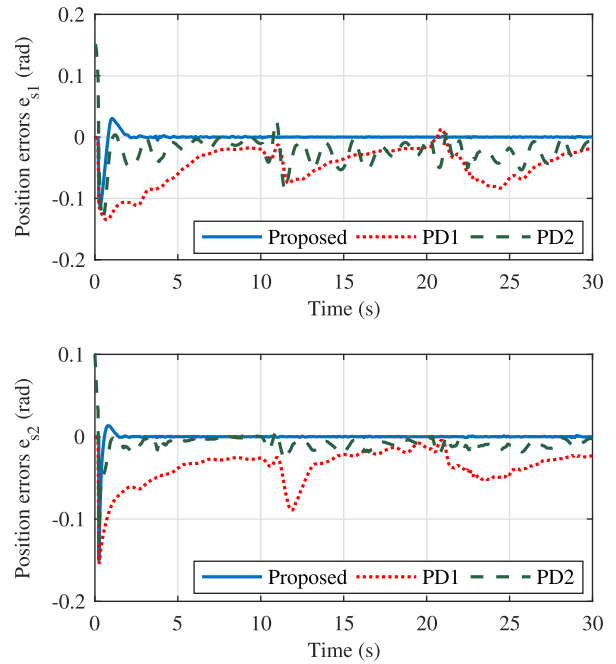


FIGURE 13. Tracking error comparison with PD control at slave side.

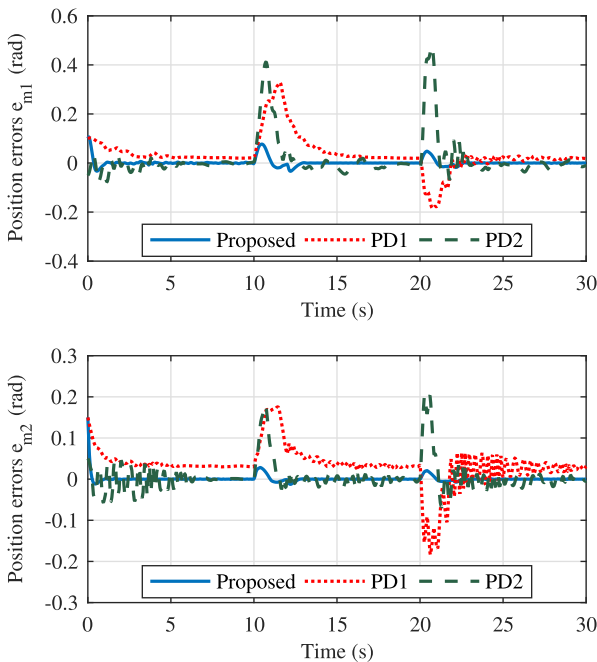


FIGURE 12. Tracking error comparison with PD control at master side.

and [35] (NTSM1 and NTSM2) and the PD methods in [31] and [36] (PD2 and PD1) are performed in this subsection.

The comparisons of tracking errors between proposed controllers, NTSM1 and NTSM2 are shown in Fig. 10 and Fig. 11. It is clearly that these three methods can converge the synchronization errors to zero in finite time. At the beginning of simulation, the proposed method and NTSM2 have the similar convergence rates, and the convergence rate of NSTM1 is the slowest. However, with

the operator force is exerted, the proposed control scheme has the better robustness and convergence performance than NTSM1 and NTSM2.

As the results, from the simulation analysis in this section, the teleoperation system can achieve well stable state and robustness with dynamic uncertainties, varying time-delay, and operator force exerted.

V. CONCLUSIONS

In this paper, considering the dynamic uncertainties and time-varying delays, the novel NTSM surface and dead zone adaptive laws are introduced into controller design. With the proposed control method, stable synchronization tracking between master and slave robots in teleoperation system is achieved, the robustness and convergence rates are also improved. And then, the simulations with proposed method and other control schemes are performed, and the effectiveness of our controllers has been verified. Moreover, the problem of oscillation in control torques need to be satisfactorily solved, and the proposed adaptive finite-time controller in this paper will be verified by experiments when the hardware platform of teleoperation system is built.

REFERENCES

- [1] L. Chan, F. Naghdy, and D. Stirling, "Application of adaptive controllers in teleoperation systems: A survey," *IEEE Trans. Human-Mach. Syst.*, vol. 44, no. 3, pp. 337–352, Jun. 2014, doi: 10.1109/THMS.2014.2303983.
- [2] P. F. Hokayem and M. W. Spong, "Bilateral teleoperation: An historical survey," *Automatica*, vol. 42, no. 12, pp. 2035–2057, Dec. 2006, doi: 10.1109/72.822511.
- [3] Z. Li, X. Cao, Y. Tang, R. Li, and W. Ye, "Bilateral teleoperation of holonomic constrained robotic systems with time-varying delays," *IEEE Trans. Instrum. Meas.*, vol. 62, no. 4, pp. 752–765, Apr. 2013, doi: 10.1109/TIM.2013.2246906.

- [4] R. Anderson and M. W. Spong, "Bilateral control of teleoperators with time delay," *IEEE Trans. Autom. Control*, vol. 34, no. 5, pp. 494–501, May 1989, doi: [10.1109/9.24201](https://doi.org/10.1109/9.24201).
- [5] G. Niemeyer and J.-J.-E. Slotine, "Stable adaptive teleoperation," *IEEE J. Ocean. Eng.*, vol. 16, no. 1, pp. 152–162, Jan. 1991, doi: [10.1109/48.64895](https://doi.org/10.1109/48.64895).
- [6] L. Hu, X. P. Liu, G. Liu, and X. P. Xu, "Trajectory tracking compensation for teleoperation with transmission delays," *Robotica*, vol. 29, no. 6, pp. 863–871, Oct. 2011, doi: [10.1017/S0263574711000075](https://doi.org/10.1017/S0263574711000075).
- [7] D. Sun, F. Naghdy, and H. Du, "Application of wave-variable control to bilateral teleoperation systems: A survey," *Annu. Rev. Control*, vol. 38, no. 1, pp. 12–31, 2014, doi: [10.1016/j.arcontrol.2014.03.002](https://doi.org/10.1016/j.arcontrol.2014.03.002).
- [8] C. Yang, X. Wang, Z. Li, Y. Li, and C.-Y. Su, "Teleoperation control based on combination of wave variable and neural networks," *IEEE Trans. Syst., Man, Cybern., Syst.*, vol. 47, no. 8, pp. 2125–2136, Aug. 2017, doi: [10.1109/TSMC.2016.2615061](https://doi.org/10.1109/TSMC.2016.2615061).
- [9] D. Sun, Q. Liao, and H. Ren, "Type-2 fuzzy modeling and control for bilateral teleoperation system with dynamic uncertainties and time-varying delays," *IEEE Trans. Ind. Electron.*, vol. 65, no. 1, pp. 447–459, Jan. 2018, doi: [10.1109/TIE.2017.2719604](https://doi.org/10.1109/TIE.2017.2719604).
- [10] Z. Li, X. Cao, and N. Ding, "Adaptive fuzzy control for synchronization of nonlinear teleoperators with stochastic time-varying communication delays," *IEEE Trans. Fuzzy Syst.*, vol. 19, no. 4, pp. 745–757, Aug. 2011, doi: [10.1109/TFUZZ.2011.2143417](https://doi.org/10.1109/TFUZZ.2011.2143417).
- [11] Z. Chen, B. Liang, and T. Zhang, "Adaptive bilateral control for nonlinear uncertain teleoperation with guaranteed transient performance," *Robotica*, vol. 34, no. 10, pp. 2205–2222, Oct. 2016, doi: [10.1017/S0263574714002847](https://doi.org/10.1017/S0263574714002847).
- [12] H. Wang, P. X. Liu, and S. Liu, "Adaptive neural synchronization control for bilateral teleoperation systems with time delay and backlash-like hysteresis," *IEEE Trans. Cybern.*, vol. 47, no. 10, pp. 3018–3026, Oct. 2017, doi: [10.1109/TCYB.2016.2644656](https://doi.org/10.1109/TCYB.2016.2644656).
- [13] T. H. Anh, N. A. Tung, N. T. Binh, D. P. Nam, and V. V. Tu, "An adaptive control law against time-varying delays in bilateral teleoperation systems," in *Proc. Int. Conf. Syst. Sci. Eng.*, Ho Chi Minh City, Vietnam, Jul. 2017, pp. 520–524.
- [14] Y. Li, Y. Yin, and D. Zhang, "Adaptive task-space synchronization control of bilateral teleoperation systems with uncertain parameters and communication delays," *IEEE Access*, vol. 6, pp. 5740–5748, 2018, doi: [10.1109/ACCESS.2018.2789864](https://doi.org/10.1109/ACCESS.2018.2789864).
- [15] S. Al-Wais, S. Khoo, T. H. Lee, L. Shanmugam, and S. Nahavandi, "Robust H-infinity cost guaranteed integral sliding mode control for the synchronization problem of nonlinear tele-operation system with variable time-delay," *ISA Trans.*, vol. 72, pp. 25–36, Jan. 2018, doi: [10.1016/j.isatra.2017.10.009](https://doi.org/10.1016/j.isatra.2017.10.009).
- [16] C. C. Hua and X. P. X. Liu, "A new coordinated slave torque feedback control algorithm for network-based teleoperation systems," *IEEE/ASME Trans. Mechatronics*, vol. 18, no. 2, pp. 764–774, Apr. 2013, doi: [10.1109/TMECH.2012.2185506](https://doi.org/10.1109/TMECH.2012.2185506).
- [17] E. Delgado, M. Diaz-Cacho, D. Bustelo, and A. Barreiro, "Generic approach to stability under time-varying delay in teleoperation: Application to the position-error control of a gantry crane," *IEEE/ASME Trans. Mechatronics*, vol. 18, no. 5, pp. 1581–1591, Oct. 2013, doi: [10.1109/TMECH.2012.2208758](https://doi.org/10.1109/TMECH.2012.2208758).
- [18] P. Yi, A. G. Song, J. H. Guo, Y. Q. Liu, and G. H. Jiang, "Delay-dependent stabilization control for asymmetric bilateral teleoperation systems with time-varying delays," in *Proc. Int. Conf. Robot. Automat. Eng.*, Jeju Island, South Korea, Aug. 2016, pp. 10–16.
- [19] M. D. Tran and H. J. Kang, "Adaptive terminal sliding mode control of uncertain robotic manipulators based on local approximation of a dynamic system," *Neurocomputing*, vol. 228, pp. 231–240, Mar. 2017, doi: [10.1016/j.neucom.2016.09.089](https://doi.org/10.1016/j.neucom.2016.09.089).
- [20] S. T. Venkataraman and S. Gulati, "Control of nonlinear systems using terminal sliding modes," *J. Dyn. Syst., Meas., Control*, vol. 115, no. 3, pp. 554–560, 1993, doi: [10.1115/1.2899138](https://doi.org/10.1115/1.2899138).
- [21] Y. Feng, X. Yu, and Z. Man, "Non-singular terminal sliding mode control of rigid manipulators," *Automatica*, vol. 38, no. 12, pp. 2159–2167, 2002, doi: [10.1016/S0005-1098\(02\)00147-4](https://doi.org/10.1016/S0005-1098(02)00147-4).
- [22] S. Yu, X. Yu, B. Shirinzadeh, and Z. Man, "Continuous finite-time control for robotic manipulators with terminal sliding mode," *Automatica*, vol. 41, no. 11, pp. 1957–1964, Nov. 2005, doi: [10.1016/j.automatica.2005.07.001](https://doi.org/10.1016/j.automatica.2005.07.001).
- [23] S. Mondal and C. Mahanta, "Adaptive second order terminal sliding mode controller for robotic manipulators," *J. Franklin Inst.-Eng. Appl. Math.*, vol. 351, no. 4, pp. 2356–2377, Apr. 2014, doi: [10.1016/j.franklin.2013.08.027](https://doi.org/10.1016/j.franklin.2013.08.027).
- [24] S. S. Mahya, A. S. Farokh, H. A. Talebi, and F. Towhidkhan, "A sliding-mode controller for dual-user teleoperation with unknown constant time delays," *Robotica*, vol. 31, no. 4, pp. 589–598, Jul. 2013, doi: [10.1017/S0263574712000604](https://doi.org/10.1017/S0263574712000604).
- [25] Y. N. Yang, C. C. Hua, H. F. Ding, and X. P. Guan, "Finite-time coordination control for networked bilateral teleoperation," *Robotica*, vol. 33, no. 2, pp. 451–462, Feb. 2015, doi: [10.1017/S026357471400037X](https://doi.org/10.1017/S026357471400037X).
- [26] Y. Yang, C. Hua, and X. Guan, "Finite time control design for bilateral teleoperation system with position synchronization error constrained," *IEEE Trans. Cybern.*, vol. 46, no. 3, pp. 609–619, Mar. 2016, doi: [10.1109/TCYB.2015.2410785](https://doi.org/10.1109/TCYB.2015.2410785).
- [27] Y. N. Yang, C. C. Hua, J. P. Li, and X. P. Guan, "Finite-time output-feedback synchronization control for bilateral teleoperation system via neural networks," *Inf. Sci.*, vol. 406, pp. 216–233, Sep. 2017, doi: [10.1016/j.ins.2017.04.034](https://doi.org/10.1016/j.ins.2017.04.034).
- [28] M. Asif, M. J. Khan, and A. Y. Memon, "Integral terminal sliding mode formation control of non-holonomic robots using leader follower approach," *Robotica*, vol. 35, no. 7, pp. 1473–1487, Jul. 2017, doi: [10.1017/S0263574716000230](https://doi.org/10.1017/S0263574716000230).
- [29] L. Zhao, H. Zhang, Y. N. Yang, and H. J. Yang, "Integral sliding mode control of a bilateral teleoperation system based on extended state observers," *Int. J. Control Automat. Syst.*, vol. 15, no. 5, pp. 2118–2125, Oct. 2017, doi: [10.1007/s12555-016-0441-8](https://doi.org/10.1007/s12555-016-0441-8).
- [30] Y. C. Liu and M. H. Khong, "Adaptive control for nonlinear teleoperators with uncertain kinematics and dynamics," *IEEE/ASME Trans. Mechatronics*, vol. 20, no. 5, pp. 2550–2562, Oct. 2015, doi: [10.1109/TMECH.2015.2388555](https://doi.org/10.1109/TMECH.2015.2388555).
- [31] S. Seshagiri and H. K. Khalil, "Output feedback control of nonlinear systems using RBF neural networks," *IEEE Trans. Neural Netw.*, vol. 11, no. 1, pp. 69–79, Jan. 2000, doi: [10.1109/72.822511](https://doi.org/10.1109/72.822511).
- [32] X. L. Xie, Z. G. Hou, L. Cheng, C. Jin, M. Tan, and H. Yu, "Adaptive neural network tracking control of robot manipulators with prescribed performance," *Proc. Inst. Mech. Eng. I-J. Syst. Control Eng.*, vol. 225, no. 16, pp. 790–797, Sep. 2011, doi: [10.1177/0959651811398853](https://doi.org/10.1177/0959651811398853).
- [33] Y. N. Y. Yang, C. C. Hua, and X. P. Guan, "Finite-time synchronization control for bilateral teleoperation under communication delays," *Robot. Comput. Integr. Manuf.*, vol. 31, pp. 61–69, Feb. 2015, doi: [10.1016/j.rcim.2014.07.001](https://doi.org/10.1016/j.rcim.2014.07.001).
- [34] J. K. Liu, "Adaptive sliding mode RBF neural network control," in *Intelligent Control Design and MATLAB Simulation*. Singapore: Springer, 2018, p. 203.
- [35] V. Panwar, "Wavelet neural network-based H-infinity trajectory tracking for robot manipulators using fast terminal sliding mode control," *Robotica*, vol. 35, no. 7, pp. 1488–1503, Jul. 2017, doi: [10.1017/S0263574716000278](https://doi.org/10.1017/S0263574716000278).
- [36] A. Forouzantabar, H. A. Talebi, and A. K. Sedigh, "Adaptive neural network control of bilateral teleoperation with constant time delay," *Nonlinear Dyn.*, vol. 67, no. 2, pp. 1123–1134, Jan. 2012, doi: [10.1007/s11071-011-0057-8](https://doi.org/10.1007/s11071-011-0057-8).

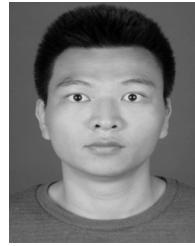


HAOCHEN ZHANG received the B.S. degree in automatic control from Southeastern University, Shenyang, China, in 2009, and the M.S. degree in control theory and control engineering from the Lanzhou University of Technology, Lanzhou, China, in 2013. He is currently pursuing the Ph.D. degree with the School of Instrument Science and Engineering, Southeast University, Nanjing, China. His current research interests are teleoperation control and robot control.



AIGUO SONG (M'98–SM'12) received the B.S. degree in automatic control and the M.S. degree in measurement and control from the Nanjing University of Aeronautics and Astronautics, Nanjing, China, in 1990 and 1993, respectively, and the Ph.D. degree in measurement and control from Southeast University, Nanjing, in 1998. He was an Associate Researcher with the Intelligent Information Processing Laboratory, Southeast University, where he was an Associate Professor with the

Department of Instrument Science and Engineering from 1998 to 2000 and the Director of the Robot Sensor and Control Laboratory from 2000 to 2003. From 2003 to 2004, he was a Visiting Scientist with the Laboratory for Intelligent Mechanical Systems, Northwestern University, Evanston, IL, USA. He is currently a Professor with the School of Instrument Science and Engineering, Southeast University. His major interests concentrate on teleoperation control, haptic display, Internet telerobotics, and distributed measurement systems.



SHAOBO SHEN received the M.S. degree in control theory and control engineering from the Nanjing University of Aeronautics and Astronautics, Nanjing, China, in 2016. He is currently pursuing the Ph.D. degree with the School of Instrument Science and Engineering, Southeast University, Nanjing. His current research interests are teleoperation control and nonlinear system control.

...